Volume 1, Number 1 (March, 2008) p. 58 - 83 • ISSN 1983-4195
REVISTA IBRACON DE ESTRUTURAS E MATERIAIS
IBRACON STRUCTURES AND MATERIALS JOURNAL

Three-dimensional analysis of reinforced concrete members via embedded discontinuity finite elements

Análise tridimensional de elementos estruturais de concreto armado via elementos finitos com descontinuidades incorporadas




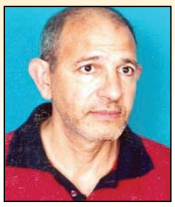

O. L. MANZOLI [a]
omanzoli@feb.unesp.br

J. OLIVER [b]
oliver@cimne.upc.es

G. DIAZ [c]
gdiaz@cimne.upc.es

A. E. HUESPE [d]
ahuespe@intec.unl.edu.ar

Abstract

This paper presents a methodology to model three-dimensional reinforced concrete members by means of embedded discontinuity elements based on the Continuous Strong Discontinuous Approach (CSDA). Mixture theory concepts are used to model reinforced concrete as a 3D composite material constituted of concrete with long fiber bundles (rebars) oriented in different directions embedded in it. The effects of the rebars are provided by phenomenological constitutive models designed to reproduce the axial non-linear behavior, as well as bond-slip and dowel action. This paper is focused on the constitutive models assumed for the components and the compatibility conditions chosen to constitute the composite. Numerical analyses of existing experimental reinforced concrete members are presented, illustrating the applicability of the methodology.

Keywords: finite elements, fracture mechanics, strong discontinuities, mixture theory, embedded cracks.

Resumo

Apresenta-se uma metodologia para modelar elementos estruturais de concreto armado tridimensionais através de elementos finitos com descontinuidade incorporada no contexto da aproximação contínua de descontinuidades fortes. Utilizam-se conceitos de teoria de misturas para representar o concreto armado como um material composto de matriz (concreto) com feixes de fibras (barras de aço) longas em diferentes direções. O efeito das barras é proporcionado por modelos constitutivos fenomenológicos, desenvolvidos para reproduzir o comportamento axial não-linear, assim como efeitos provenientes de deslizamento por perda de aderência e ação de pino. O presente artigo foca os modelos constitutivos dos componentes e as condições de compatibilidade escolhidas para constituir o composto. Para ilustrar a aplicabilidade da metodologia proposta, apresentam-se análises numéricas de testes experimentais de elementos de concreto armado existentes.

Palavras-chave: elementos finitos, mecânica de fratura, descontinuidades fortes, teoria de misturas, fissuras incorporadas.

[a] *Departamento de Engenharia Civil, Universidade Estadual Paulista, Bauru, SP, Brasil, e-mail: omanzoli@feb.unesp.br*
[b] *Universidad Politécnica de Cataluña (UPC), Barcelona, España, e-mail: oliver@cimne.ups.es*
[c] *Universidad Politécnica de Cataluña (UPC), Barcelona, España, e-mail: gdiaz@cimne.ups.es*
[d] *CIMEC/Intec, Conicet, Santa Fe, Argentina, e-mail: ahuespe@intec.unl.edu.ar*

1. Introduction

The mechanical behavior of reinforced concrete members is strongly affected by the damage caused by the formation of cracks during the loading process. In many situations, the ultimate load capacity corresponds to a collapse mechanism caused by the formation of one or a few dominant cracks that appear when the concrete is already highly degraded by previous cracks. Therefore, in order to model the reinforced concrete behavior, it is fundamental an approach able to describe the formation and propagation of multiple cracks in non-homogenous solids composed of concrete and steel bars.

Finite elements with embedded strong discontinuities have acquired great relevance, in modeling fracturing processes, mainly due to the increase in robustness and stability that they provide in comparison with other methods. The development of an effective technique to track multiple discontinuity paths in two and three dimensional solids, based on an analogous thermal problem, also stands out [1, 2]. With these advances, this finite element class currently exhibits maturity to represent the complex crack growth process in reinforced concrete, so long as the effects of the steel bars are also appropriately included. These effects must reflect the contribution provided by the mechanical behavior of the steel bars, as well as the interaction phenomena between concrete and reinforcement, related to bond-slip and dowel actions.

There are different possibilities to take these effects into account. A *mesoscopic* scale treatment could be adopted, using homogenous solid elements of concrete and reinforcement with interfacing elements between them to model the bonding behavior. However, when practical problems of reinforced concrete structures are focused, this mesoscopic treatment requires, many times, unaffordable computational costs. Therefore, an alternative is a *macroscopic* scale treatment, where, the steel bars are considered embedded in the solid elements, permitting the use of coarse meshes and thus reducing computational efforts.

In this sense, the mixture theory [3] is a suitable option for modeling reinforcement at this macroscopic level. Using this theory, the effects of the fibers (steel bars) at the mesoscopic level can be added to the matrix (concrete) behavior at the macroscopic level resulting in an equivalent homogenized material. For the long fibers case, as is the case of steel reinforcement bars, a parallel mechanical mixture option can be employed, assuming that all constituents share the same strain field (or specific components of it). Then, the composite stress field can be obtained by the sum of the stresses supplied by the constitutive model of each constituent, weighted according to its corresponding volumetric fraction. In order to formulate these constitutive models, one can resort to available phenomenological models based on standard continuum theories. In this case, the Continuum Strong Discontinuity Approach (CSDA) can be used to model material failure of the composite. The resulting methodology, which combines the CSDA with the mixture theory, was initially proposed by Linero [4] for two-dimensional analyses of reinforced concrete members with two orthogonal bundles of fibers, which led to very promising results.

The present study extends this methodology, already presented for 2D problems in [7], to three-dimensional problems with an unlimited number of fiber bundles in different directions. The matrix and each fiber bundle are treated as constituents of the composite, which in turn, can be regarded as a homogenous continuum. Thus, the numerical simulation of the formation and propagation of cracks can be carried out by using finite elements with embedded strong discontinuities, within the context of the CSDA, like in homogeneous continua, where application of that approach has already been extensively studied [2, 5, 6].

Therefore this work is focused on the representation of the constitutive models used to describe the mechanical behavior of the constituents, as well as the compatibility conditions used to form the composite material and provide the phenomenological effects related to the interaction between concrete and steel bars.

Figure 1 – (a) Composite material with one discontinuity, (b) representative material point

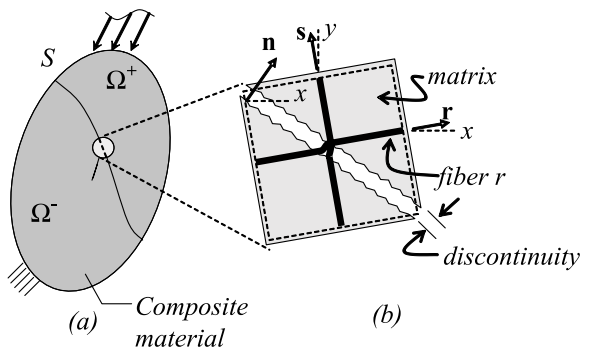

2. Composite material

Reinforced concrete is assumed a composite material made of a matrix (concrete) and long fibers (steel bars) arranged in different directions, as shown in Figure 1. According to the basic hypothesis of the mixture theory, the composite is a continuum in which each infinitesimal volume is occupied by all the constituents [3]. Assuming a parallel layout, all constituents are submitted to the composite deformation. The composite stresses are obtained by summing up the stresses of each constituent, weighted according to their corresponding volumetric participation. Thus, the matrix strains, $\boldsymbol{\varepsilon}^m$, coincide with the composite strains, $\boldsymbol{\varepsilon}$:

$$\boldsymbol{\varepsilon}^m = \boldsymbol{\varepsilon} \tag{1}$$

The extensional strain of a fiber *f*, in direction $\mathbf{r}^{(f)}$, is equal to the component of the composite strain field in that direction, that is:

$$\varepsilon^{(f)} = \mathbf{r}^{(f)} \cdot \boldsymbol{\varepsilon} \cdot \mathbf{r}^{(f)} \tag{2}$$

As it will be shown later, in order to take dowel action into consideration, the fiber shear strains, $\gamma^{(f)}$, are obtained as the shear components of the composite strain field. In a local orthogonal reference system $(\mathbf{r}^{(f)},\mathbf{s}^{(f)},\mathbf{t}^{(f)})$ these shear components are given by:

$$\gamma_{rs}^{(f)} = 2\mathbf{r}^{(f)}\cdot\varepsilon\cdot\mathbf{s}^{(f)} \tag{3}$$

$$\gamma_{rt}^{(f)} = 2\mathbf{r}^{(f)}\cdot\varepsilon\cdot\mathbf{t}^{(f)} \tag{4}$$

The stresses of a composite with *nf* fibers (or fiber bundles) oriented in different directions $\mathbf{r}^{(f)}$ (*f*=1,2,..,*nf*) can be obtained using the following weighted sum of each contribution:

$$\sigma = k^m\sigma^m(\varepsilon^m)+\sum_{f=1}^{nf}k^{(f)}\left\{\sigma^{(f)}(\varepsilon^{(f)})\left(\mathbf{r}^{(f)}\otimes\mathbf{r}^{(f)}\right)+ +2\tau_{rs}^{(f)}(\gamma_{rs}^{(f)})\left(\mathbf{r}^{(f)}\otimes\mathbf{s}^{(f)}\right)^s+2\tau_{rt}^{(f)}(\gamma_{rt}^{(f)})\left(\mathbf{r}^{(f)}\otimes\mathbf{t}^{(f)}\right)^s\right\} \tag{5}$$

where k^m and $k^{(f)}$, are the matrix and the fiber *f* volumetric fraction, respectively, σ^m is the matrix stress tensor, $\sigma^{(f)}$ is the fiber normal (axial) stress, and $\tau_{rs}^{(f)}$ and $\tau_{rt}^{(f)}$ are the shear stress components. For the sake of simplicity, in Equation (5), it was assumed that the normal and tangential stress components of the fibers are related to the corresponding strains by means of specific constitutive equations in a completely decoupled manner.
Since the composite stresses are obtained from the composite strains, the incremental form of the composite constitutive equation can be written as:

$$\dot{\sigma} = \mathbf{C}_{tg}:\dot{\varepsilon} \tag{6}$$

where the tangent constitutive tensor $\mathbf{C}_{tg}$ can be obtained from the incremental form of Equation (5), as:

$$\mathbf{C}_{tg} = k^m\mathbf{C}_{tg}^m+\sum_{f=1}^{nf}k^f\left\{E_{tg}^{(f)}\left(\mathbf{r}^{(f)}\otimes\mathbf{r}^{(f)}\right)\otimes\left(\mathbf{r}^{(f)}\otimes\mathbf{r}^{(f)}\right)+ +4G_{rs}^{(f)}\left(\mathbf{r}^{(f)}\otimes\mathbf{s}^{(f)}\right)^s\otimes\left(\mathbf{r}^{(f)}\otimes\mathbf{s}^{(f)}\right)^s+4G_{rt}^{(f)}\left(\mathbf{r}^{(f)}\otimes\mathbf{t}^{(f)}\right)^s\otimes\left(\mathbf{r}^{(f)}\otimes\mathbf{t}^{(f)}\right)^s\right\} \tag{7}$$

in which $\mathbf{C}_{tg}^m=\partial\boldsymbol{\sigma}^m/\partial\boldsymbol{\varepsilon}$, $E_{tg}^{(f)}=\partial\sigma^{(f)}/\partial\varepsilon^{(f)}$, $G_{rs}^{(f)}=\partial\tau_{rs}^{(f)}/\partial\gamma_{rs}^{(f)}$ e $G_{rt}^{(f)}=\partial\tau_{rt}^{(f)}/\partial\gamma_{rt}^{(f)}$ are the tangent operators for the involved constitutive relations.

3. The Continuum Strong Discontinuity Approach (CSDA)

Crack onset and growth in the composite can be modeled in the context of the CSDA, originally proposed by Simó et al. [7]. Descriptions of the CSDA, as well as the details of its implementation in the context of finite elements with embedded discontinuities, can be found in references [8-11]. In order to increase robustness during the non-linear computations, a symmetric formulation (kinematically consistent) combined with an implicit-explicit integration scheme presented in reference [6] are used. Continuity of the crack paths between finite elements (2D and 3D) is imposed by a global tracking algorithm based on an analogous thermal problem [1].
For the numerical examples presented here, the failure orientation was assumed as being the maximum principal stress direction, evaluated when the discontinuous bifurcation condition [10] for this direction is reached.

4. Constitutive models

4.1 Constitutive model for the concrete matrix

The constitutive behavior of the concrete matrix is described through an isotropic damage model with distinct tensile and compressive strengths. This model belongs to the family of damage models proposed by Simo and Ju [12] and presented by Oliver et al. [13].
The model is governed by the following equations:

$$\sigma^m=\frac{q}{r}\bar{\sigma}^m\ ;\ \bar{\sigma}^m=\mathbf{C}^m:\varepsilon^m\quad\text{(constitutive relation)} \tag{8}$$

$$f(\varepsilon^m,r)=\tau_\varepsilon-r\le 0\ ;\quad \tau_\varepsilon=\alpha\sqrt{\bar{\sigma}^m:(\mathbf{C}^m)^{-1}:\bar{\sigma}^m}=\alpha\sqrt{\varepsilon^m:\mathbf{C}^m:\varepsilon^m}\quad\text{(damage criterion)} \tag{9}$$

$$\dot{q}=H^m\dot{r}\quad\text{(softening law)} \tag{10}$$

$$r(t)=\max_{s\in[0,t]}\left[r_0,\tau_\varepsilon(s)\right]\ ;\ r_0=\frac{\sigma_u^m}{\sqrt{E^m}}\quad\text{(evolution of the strain-like internal variable)} \tag{11}$$

where $\bar{\boldsymbol{\sigma}}^m$ is the effective stress tensor, $\mathbf{C}^m$ is the elastic constitutive tensor, *r* and *q* are the strain and stress-like internal variables, respectively, related in Equation (10) through the softening module H^m, σ_u^m is the tensile strength and E^m is Young's module. The α factor in the damage criterion of Equation (9) is defined as:

$$\alpha = \frac{\sum_{i=1}^{3} \left\langle \bar{\sigma}_i^m \right\rangle}{\sum_{i=1}^{3} \left| \bar{\sigma}_i^m \right|} \left(1 - \frac{1}{n} \right) + \frac{1}{n} \qquad (12)$$

where $\bar{\sigma}_i^m$ is the *i-nth* principal effective stress, $\langle \bullet \rangle$ represents the Mac-Auley operator ($\langle x \rangle = x$, if $x>0$ e $\langle x \rangle = 0$, if $x \leq 0$) and n is the concrete compressive/tensile strength ratio (see Figure 2).
The incremental form of the constitutive equation can be expressed by:

$$\dot{\sigma}^m = \mathbf{C}_{tg}^m : \dot{\varepsilon}^m \qquad (13)$$

where the tangent constitutive tensor, $\mathbf{C}_{tg}^m$, takes one of the following values, depending on the loading status:

$$\mathbf{C}_{tg}^m = \frac{q}{r}\mathbf{C}^m \text{ se } \dot{r} = 0 \text{ ; (unloading)} \qquad (14)$$

$$\mathbf{C}_{tg}^m = \frac{q}{r}\mathbf{C}^m - \left(\frac{q - H^m r}{r^3} \right) \cdot \left[\frac{r^2}{\alpha} \left(\bar{\sigma}^m \otimes \mathbf{A} \right) + \alpha^2 \left(\bar{\sigma}^m \otimes \bar{\sigma}^m \right) \right] \text{ se } \dot{r} > 0 \text{ ; (loading)} \qquad (15)$$

$$\mathbf{A} = \mathbf{C}^m : \partial_{\bar{\sigma}} \alpha$$

In order to make the constitutive model compatible with the regularized form of strong discontinuity kinematics, and with the principles of fracture mechanics, the softening module shall depend on the strain localization bandwidth, a small regularization value *k*, as well as on the fracture energy (mode I), G_f^m, considered as a material property. Thus, for the linear softening case, H^m is given by

$$H^m = \bar{H}^m k \text{ ; } \bar{H}^m = -\frac{{\sigma_u^m}^2}{2E^m G_f^m} \qquad (16)$$

4.2 Constitutive model for the steel fibers

Steel fibers (rebars) are regarded as one-dimensional elements embedded in the matrix. They can contribute to the composite mechanical behavior introducing axial or shear strength and stiffness.
The axial contribution of each fiber bundle depends on its mechanical properties and the matrix-fiber bond/slip behavior. The combination of both mechanisms is modeled by the slipping-fiber model described below. In this framework, the dowel action can be provided by the fiber shear stiffness contribution in the crack zone.

Figure 2 – Damage model: (a) damage criterion in the effective stress space, (b) one-dimensional stress-strain curve

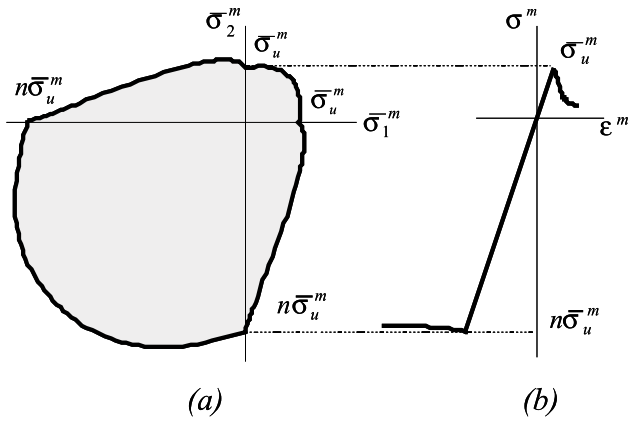

4.2.1 Slipping-fiber model

The fiber axial contribution can be modeled through one-dimensional constitutive relations, relating extensional strains with normal stresses. The assumed compatibility between matrix and fiber strains allows capturing the slip effect due to the bond degradation by means of a specific strain component associated with the slip. Thus, the fiber extensional strain, ε^f, can be assumed as a composition of two parts: one due to fiber mechanical deformation, ε^d, and the other related to the equivalent relaxation due to the bond-slip in the matrix-fiber interface, ε^i:

$$\varepsilon^f = \varepsilon^d + \varepsilon^i \qquad (17)$$

Assuming a serial composition between fiber and interface, as illustrated in Figure 3, the normal stress of the slipping-fiber model, σ^f, is equal to each component stress:

$$\sigma^f = \sigma^d = \sigma^i \qquad (18)$$

The stress associated with the fiber elongation as well as the one associated with the matrix-fiber slip effect can be related to the corresponding strain component by means of a uniaxial linearly elastic/perfectly plastic constitutive model [14]. Thus, this serial composition results in a slipping-fiber behavior, which can also be described by means of a linearly elastic, perfectly plastic model,

whose material parameters are provided by the composition of parameters associated with each effect (see figure 4). Therefore, the elastic module, E^f, and the yield stress, σ_y^f, of the slipping-fiber constitutive model are given by:

$$E^f = \frac{1}{1/E^d + 1/E^i} \quad (19)$$

$$\sigma_y^f = \min\left[\sigma_y^d, \sigma_{adh}^i\right] \quad (20)$$

where E^d and σ_y^d are the steel Young´s module and yield stress, E^i is the elastic module for the matrix-fiber interface and σ_{adh}^i is the bond stress limit.

The parameters related to the fiber axial deformation can be obtained from steel bar tension tests, whereas those related to bond can be estimated from pull-out tests.

4.2.2 Dowel action

In some situations, the so called dowel action can contribute significantly to the shear behavior of reinforced concrete members, especially in loading stages near or beyond the ultimate loads.

To take into account the dowel action produced by steel bars crossing cracks, additional shear stiffness, due to the interaction of rebars and concrete in the relative transversal shift between the crack lips has to be introduced. This shear force transfer mechanism models the interaction between the steel bars and the surrounding concrete, and can be modeled by treating the rebars as beams on an elastic foundation [15,16].

The additional stiffness is provided by the last two stress contributions in Equations (5) and (7). For the sake of simplicity, the shear stress contributions in the two planes orthogonal to the direction of the fiber bundle (**r**), τ_{rs}^f and τ_{rt}^f, can be assumed decoupled and described by a linearly elastic/perfectly plastic model, as shown in Figure 5.

The model parameters, τ_y^f and G^f, can be estimated from the mechanical properties of the concrete and steel bars, according to the model described in reference [15].

5. Numerical simulations

5.1 Panel in tension

The reinforced concrete panel subject to axial tension reported by Ouyang and coauthors [17,18] is analyzed. The specimen consists of a 686 mm x 127 mm, 50.8mm thick, panel, reinforced with three 9.5 mm in diameter steel bars, as shown in Figure 6.

The concrete mechanical properties are: E^m= 27.35 GPa, ν^m =0.2, G_f^m =100.N/m and σ_u^m =3.19 MPa. The steel bars have the following properties: E^d=191.6 GPa and σ_y^d =508.0MPa. The

Figure 3 – Slipping-fiber model

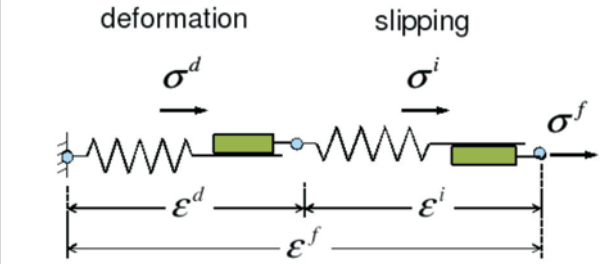

bond properties between concrete and steel bars were characterized through pull-out tests reported by Naaman et al. [19], which led to the following slipping-fiber model properties, described in section 4.2 : E^f =0.86 E^d e σ_{adh}^i = 311.1 MPa.

In order to compare the correctness of the present three dimensional approach, numerical analyses were carried out using two-dimensional (2D) and three-dimensional (3D) numerical models. The two-dimensional analysis was performed using three-node triangular finite elements to model only one fourth of the panel, taking into account the problem symmetry. For the three-dimensional analysis, one eighth of the panel was modeled using four-node tetrahedral finite elements. Figures 7 and 8 illustrate the used finite element meshes In both cases, each rebar and the surrounding concrete, indicated by the finite elements with darker colors in Figures 7 and 8, were replaced by a composite material with 8.24% and 24.71% of axial fibers for the 2D and 3D cases, respectively. The rest of the panel was modeled using plain concrete properties. Axial tension was induced by imposing an increasing axial displacements at the nodes located at the right end of the panel (see Figure 6).

Figures 9 and 10 show the iso-displacement contours for different load levels. In these figures, the concentrations of contour lines indicate the presence of strain localization associated with the crack opening inside the finite elements. Observe that, after reaching the tensile strength, the concrete begins to present cracks propagating from the external to the internal regions, until stabilization, with an almost constant spacing between them. It is important to observe that, unlike in other models, this spacing value was not introduced as a model parameter, but it emerges naturally as a *saturation crack distance* as a result of the analysis. For the three-dimensional analysis, it is possible to observe the distinct crack-opening levels at the external and internal regions (near to the bars).

The structural results (reaction force vs. imposed displacement) obtained numerically are compared with the experimental ones in Figure 11. Both the two- and three-dimensional analyses provide results similar to the experimental ones. It is important to note that the so called *tension-stiffening* effect is naturally captured without introducing any ad-hoc contributions associated with this phenomenon in the material constitutive model. Indeed, in the figure it can be checked that, even after the concrete cracking, the structural response is stiffer than the one obtained with three identical steel bars not embedded in concrete, and that this additional stiffness is here provided by the concrete between cracks.

The evolution of cracks clearly shows the distinct phases of the material degradation process. The first cracks, almost uniformly

Figure 4 – Slipping-fiber model composition

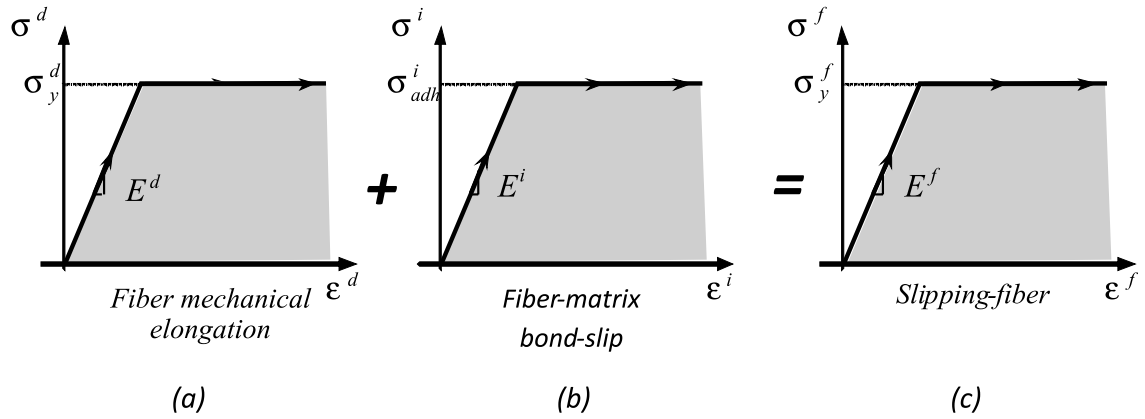

spaced, occur when concrete reaches the tensile strength. At that moment, the structural curve shows a stiffness drop produced by the rapid matrix degradation, whereas the steel bars remain in linearly elastic regime. As the imposed displacements are increased, new sets of cracks emerge, between the existing ones, until crack stabilization takes place. In this stabilized stage, the existing cracks open continuously. The ultimate load capacity is reached when the rebars yield at one of the cracked cross-sections leading to a failure mode characterized by a single active crack.

Figure 5 – Dowel action constitutive model

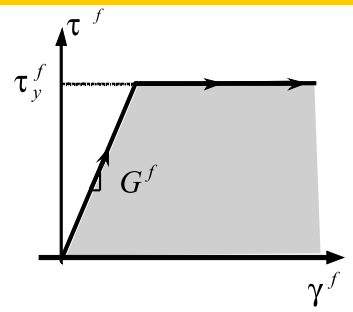

5.2 Reinforced concrete corbel

This typically 3D test, on a reinforced concrete corbel, carried out by Mehmel and Freitag [20] is analyzed numerically. The test description is given in Figure 12. Each steel bar and the surrounding concrete were modeled by a composite material with equivalent mechanical properties. The corbel was then divided into sub-regions involving the steel bars, as shown in Figure 13. In each sub-region, the fiber direction and volumetric fraction corresponds to the embedded steel bars in the real problem. The assumed mechanical properties for the concrete are: E^m= 21.87 GPa, ν^m =0.2, G_f^m =100.N/m and σ_u^m =2.26 MPa. The steel bars have the following properties: E^d=206 GPa and σ_y^d =430 MPa. The bond properties between concrete and steel bars were introduced taking into account the following slipping-fiber properties: $E^f = E^d$ and σ_{adh}^i = 300 MPa.

The iso-displacement contours at the end of the analysis, shown in Figure 14, display the

Figure 6 – Reinforce concrete panel subjected to uniaxial tension

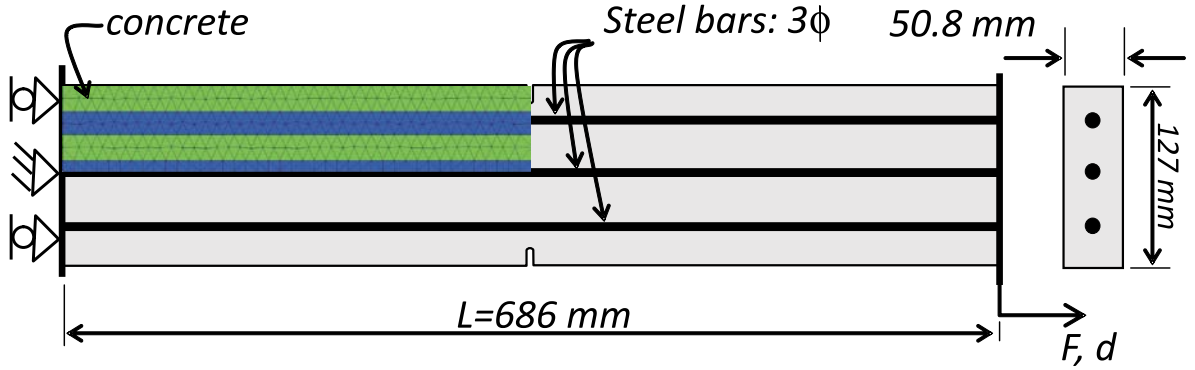

Figure 7 – Reinforce concrete panel subjected to uniaxial tension. Two-dimensional mesh

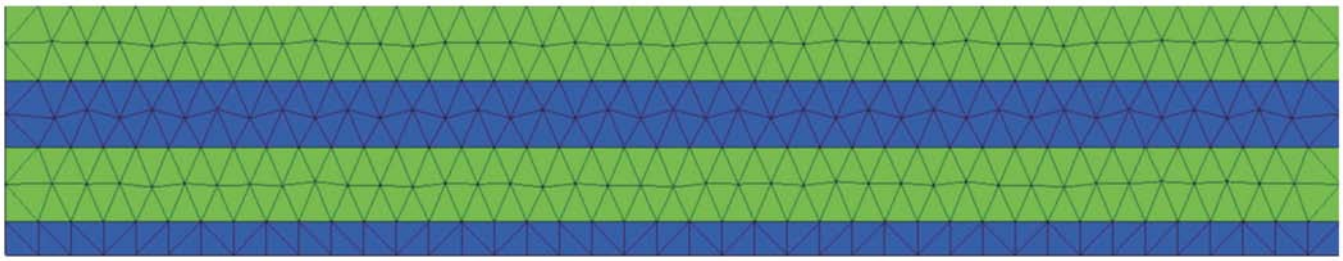

obtained crack pattern, which is in good correspondence with the one observed in the experiment.

Figure 15 compares the structural curves obtained numerically, with the proposed methodology, and the ones obtained using a model based on the smeared crack model with embedded representation of the rebars, presented by Hardtl [21]. Both methodologies provide a reasonable prediction of the experimental ultimate load capacity.

6. Conclusions

The methodology proposed to describe the behavior of reinforced concrete members is founded on the following aspects:

- Macroscopic representation of reinforced concrete by means of the mixture theory;
- Standard constitutive laws to describe each constituent behavior (concrete and steel), as well their interactions (bond-slip and dowel action);
- Continuum Strong Discontinuities Approach to describe material failure of the resulting composite material;
- Finite elements with embedded discontinuities to simulate crack propagation with a fixed mesh;
- Global 3D tracking algorithm to capture multiple crack surfaces;
- Implicit-explicit integration scheme to improve robustness and stability of non-linear computations.

With these aspects, the present methodology is able to:

- Describe the degradation process caused by the formation of multiple cracks;
- Reproduce the tension-stiffening effect provided by the

Figure 8 – Reinforce concrete panel subjected to uniaxial tension. Three-dimensional mesh

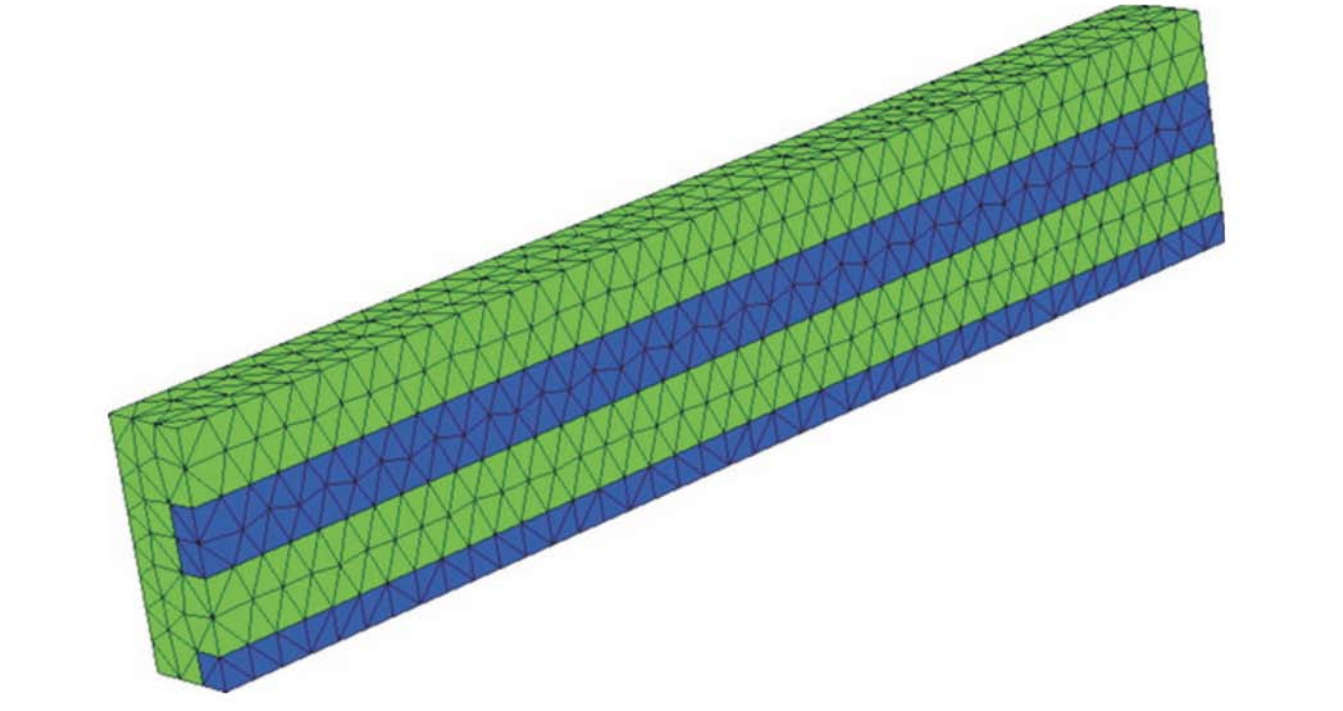

concrete behavior between cracks, without the need of specific models for this;
- Take into account bond-slip effects between steel bars and concrete;
- Provide additional shear stiffness associated with dowel action.

Figure 9 – Two-dimensional numerical results. Iso-displacement contours for different imposed displacement levels

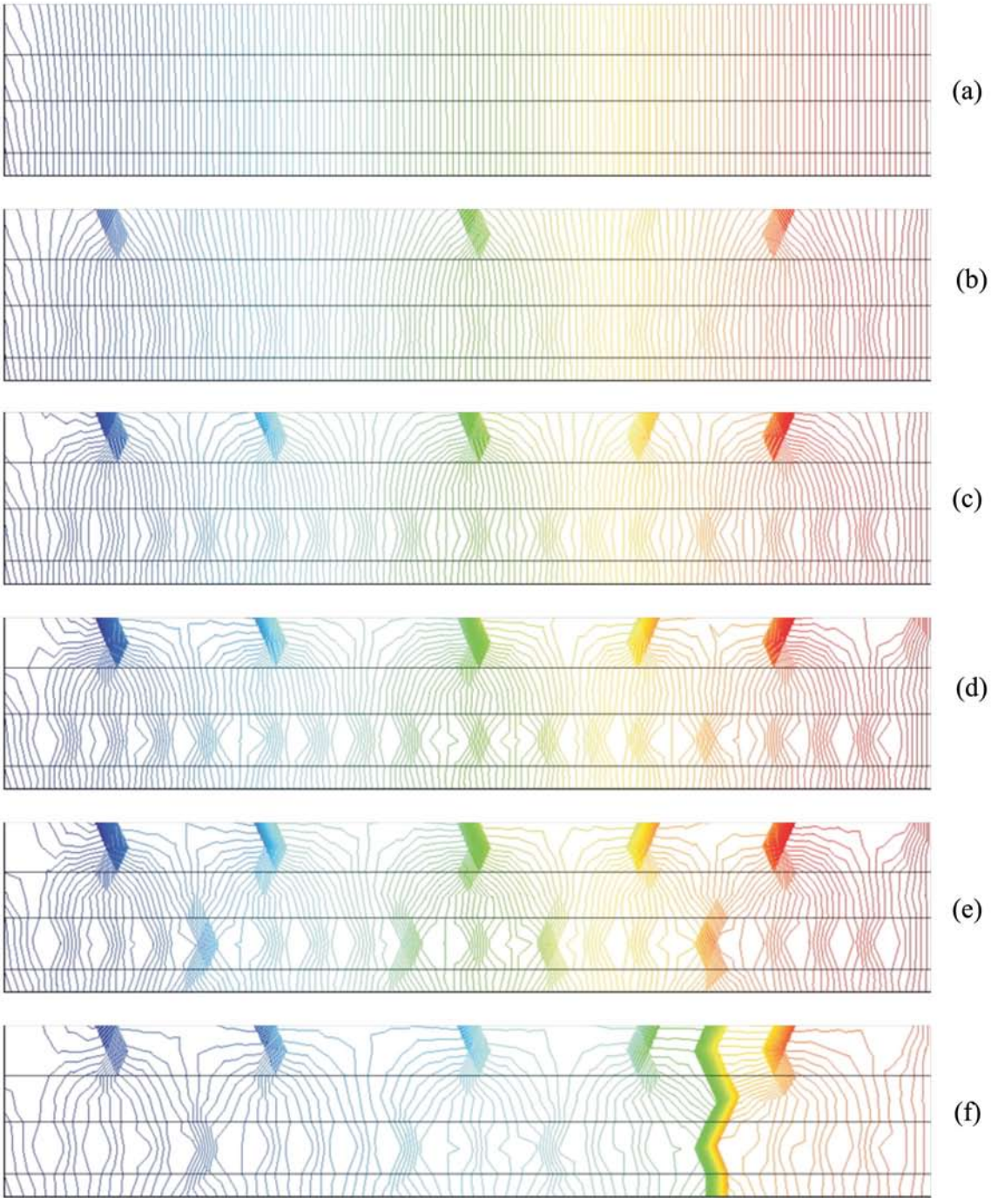

The proposed approach intends to be an alternative tool to deal with the complex physical phenomena with minimal computational effort. For this purpose, the mixture theory is used to include the reinforcement effects in a macroscopic scale, avoiding an explicit representa-

Figure 10 – Three-dimensional numerical results. Iso-displacement contours for different imposed displacement levels

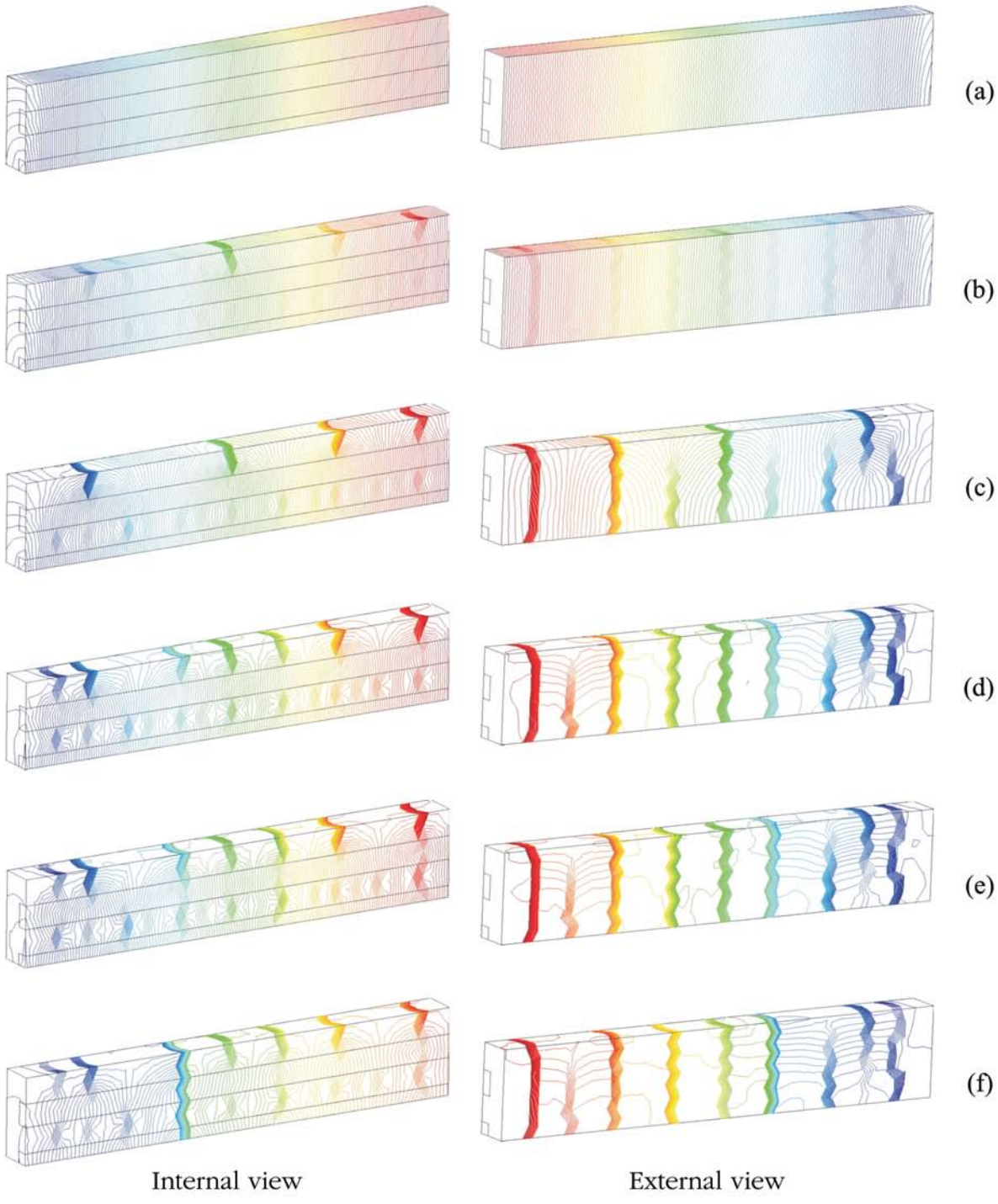

tion of each reinforcement bar in a mesoscopic context.
On the other hand, the continuum strong discontinuity approach allows for modeling the mechanical behavior of all the composite constituents (concrete and rebars), as well as the involved dominant phenomena (multiple cracks, bond slip and tension stiffening), in a simple manner via standard stress-strain constitutive models.

Figure 11 – Reinforce concrete panel. Reaction force vs imposed displacement responses

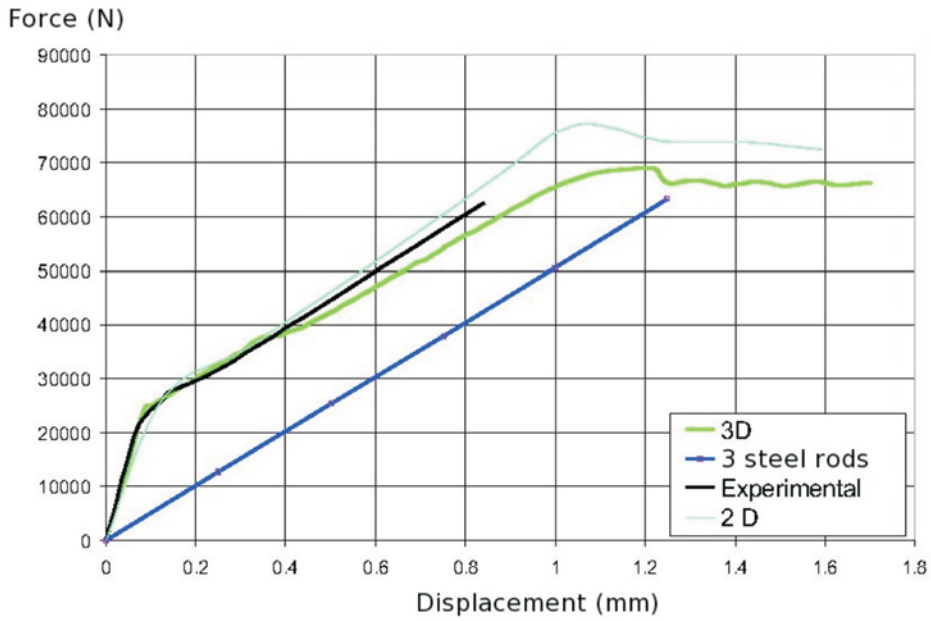

Figure 12 – Reinforced concrete corbel

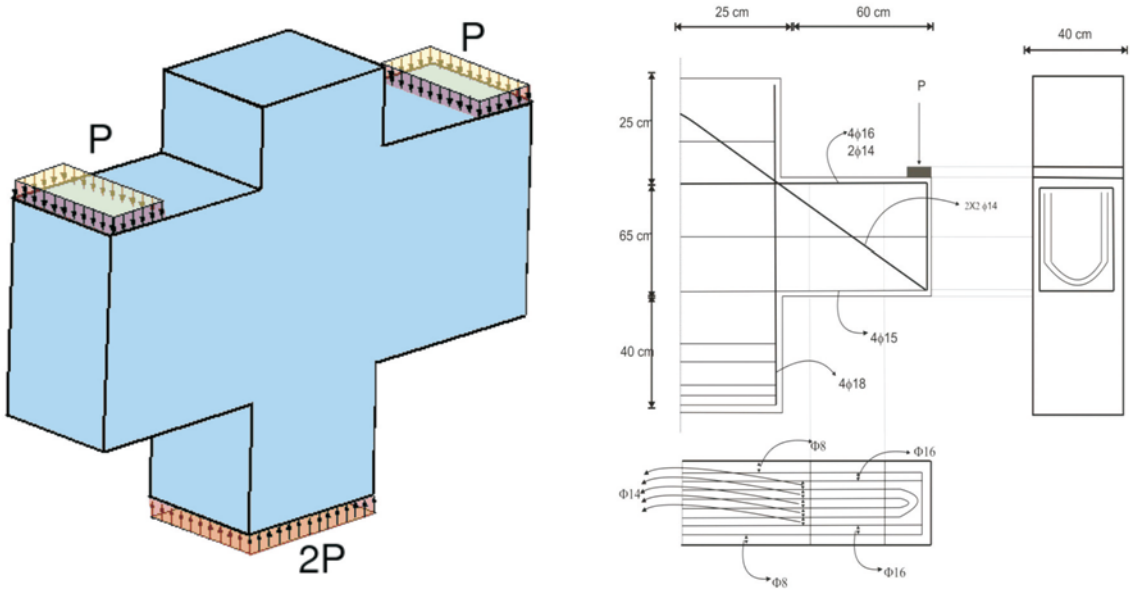

The combination of those models with the strong discontinuity kinematics in the CSDA, numerically captured by finite elements with embedded discontinuities, projects those continuum models into a, presumably, very complex traction separation laws, which are fulfilled at the cracks but that are never derived

This kind of approach is advantageous for three-dimensional numerical simulations, requiring finite element sizes lager than those necessary in mesoscopic approaches where the actual geometry of the rebar cross section has to be represented. Here bundles or layers of rebars, surrounded by appropriated amounts of concrete,

Figure 13 – Reinforced concrete corbel. Four-node tetrahedral finite element mesh

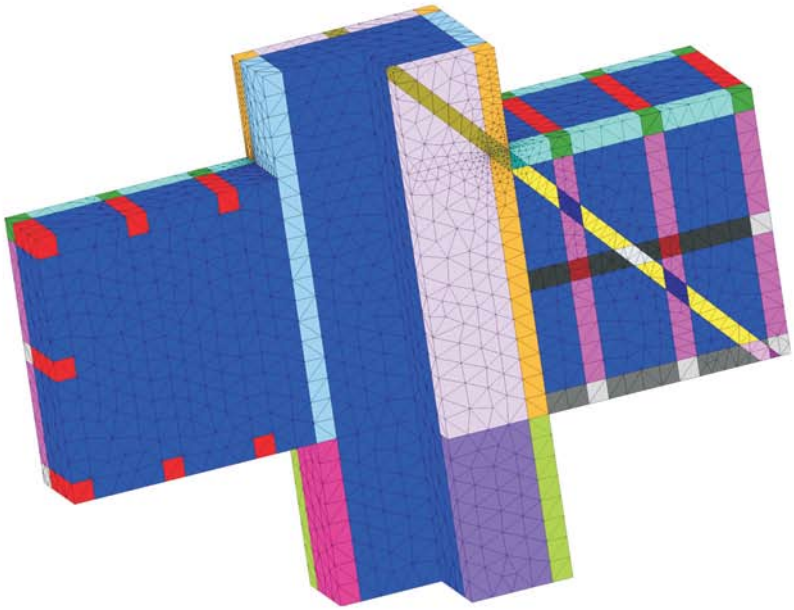

Figure 14 – Reinforced concrete corbel. Crack patterns

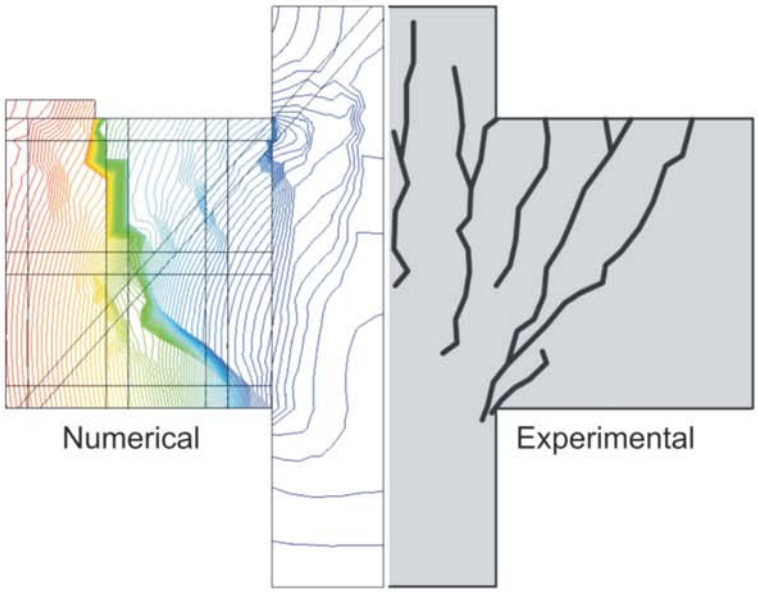

are modeled as composite materials whose size determines the finite element mesh. Therefore, the required computational cost drops dramatically with respect to mesoscopic approaches.
On the other hand, as it has been displayed by the presented results, that simplification in the geometry does not translate into a significant loss of quality of the obtained mechanical description of the reinforced concrete members. Crack patterns, failure mechanisms and action-response curves coincide, with remarkable accuracy, with the ones displayed experiments.

7. REFERÊNCIAS

[01] Oliver, J., et al., *Continuum approach to the numerical simulation of material failure in concrete.* International Journal for Numerical and Analytical Methods in Geomechanics, 2004. **28**(7-8): p. 609-632.

[02] Oliver, J. and A.E. Huespe, *Continuum approach to material failure in strong discontinuity settings.* Computer Methods in Applied Mechanics and Engineering, 2004. **193**(30-32): p. 3195-3220.

[03] Trusdell, C. and R. Toupin, *The classical field theories. Handbuch der Physik III/I*. 1960, Berlin: Springer Verlag.

[04] Linero, D.L., *Un modelo de fallo material en el hormigón armado mediante la metodología de discontinuidades fuertes de continuo y la teoría de mezclas*. 2006, Universidad Politécnica de Cataluña: Barcelona.

[05] Blanco, S., et al. *Strong discontinuity modeling of material failure in large concrete structures: recent computational developments and applications*. in *EURO-C 2006 Computational Modelling of Concrete Structures*. 2006. Tyrol (Austria): Balkema Publishers.

[06] Oliver, J., et al., *Stability and robustness issues in numerical modeling of material failure in the strong discontinuity approach.* Comput. Methods Appl. Mech. Engng., 2006. **195**: p. 7093-7114.

[07] Simo, J., J. Oliver, and F. Armero, *An analysis of strong discontinuities induced by strain-softening in rate-independent inelastic solids.* Computational Mechanics, 1993. **12**: p. 277-296.

[08] Oliver, J., *Modelling strong discontinuities in solid mechanics via strain softening constitutive equations .1. Fundamentals.* International Journal for Numerical Methods in Engineering, 1996. **39**(21): p. 3575-3600.

[09] Oliver, J. and A.E. Huespe, *Theoretical and computational issues in modelling material failure in strong discontinuity scenarios.* Computer Methods in Applied Mechanics and Engineering, 2004. **193**(27-29): p. 2987-3014.

[10] Oliver, J., M. Cervera, and O. Manzoli, *Strong discontinuities and continuum plasticity models: the strong discontinuity approach.* International Journal of Plasticity, 1999. **15**(3): p. 319-351.

[11] Manzoli, O.L. and P.B. Shing, *A general technique to embed non-uniform discontinuities into standard*

Figure 15 – Reinforced concrete corbel. Reaction force vs displacement responses

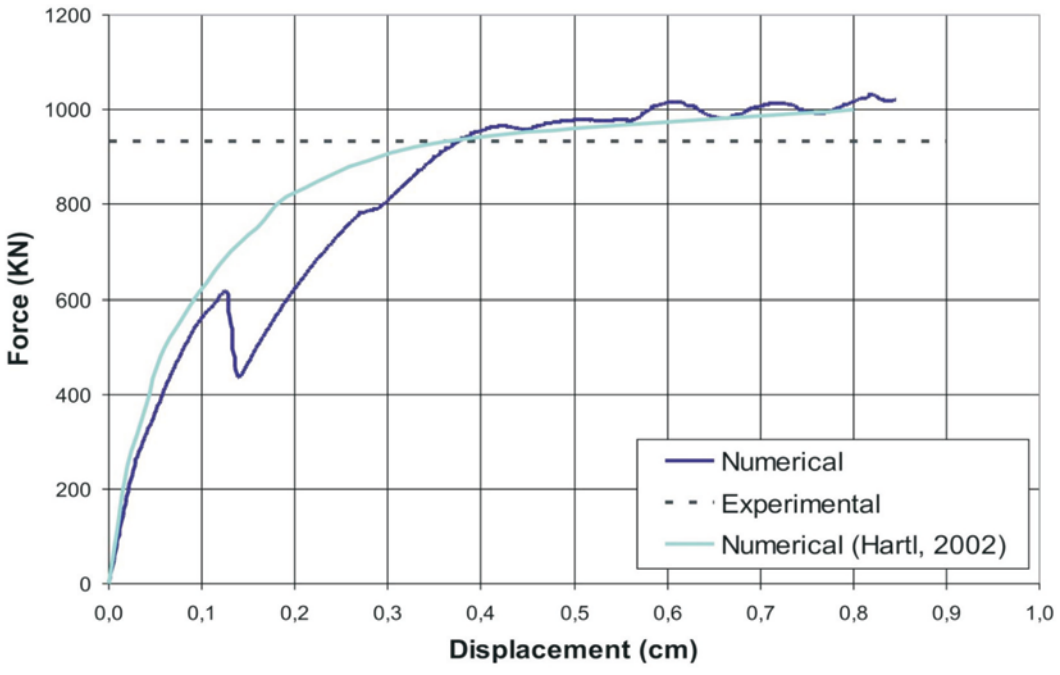

solid finite elements. Computers & Structures, 2006. **84**(10-11): p. 742-757.

[12] Simo, J.C. and J.W. Ju, *Stress and strain based continuum damage models: I formulation.* International Journal Solids and Structures, 1987. **15**: p. 821-840.

[13] Oliver, J., et al. *Isotropic damage models and smeared crack analysis of concrete*. in *Proc. SCI-C Computer Aided Analysis and Design of Concrete Structures*. 1990.

[14] Simo, J.C. and T.J.R. Hughes, *Computational Inelasticity*. 1998: Springer.

[15] He, X.G. and A.K.H. Kwan, *Modeling dowel action of reinforcement bars for finite element analysis of concrete structures.* Computers & Structures, 2001. **79**(6): p. 595-604.

[16] Deipoli, S., M. Diprisco, and P.G. Gambarova, *Shear Response, Deformations, and Subgrade Stiffness of a Dowel Bar Embedded in Concrete.* Aci Structural Journal, 1992. **89**(6): p. 665-675.

[17] Ouyang, C., et al., *Prediction of cracking response of reinforced concrete tensile members.* Journal of Structural Engineering. ASCE, 1997. **123**(1): p. 70 - 78.

[18] Ouyang, C. and P. Shah, *Fracture energy approach for predicting cracking of reinforced concrete tensile members.* ACI Structural Journal, 1994. **91**(1): p. 69-78.

[19] Naaman, A., et al., *Fiber pullout and bond slip II. Experimental validation.* Journal of Structural Engineering ASCE, 1991. **117**(9): p. 2791-2800.

[20] Mehmel, A. and W. Freitag, *Tragfahigkeitsversuche an Stahlbetonkonsolen.* Bauingenieur, 1967. **42**: p. 362-369.

[21] Hartl, H., *Development of a continuum-mechanics-based toll for 3D finite element analysis of reinforced concrete structures and application to problems of soil-structure interaction*. 2002, Graz University of Technology: Graz.